Supplementary Information

Theoretical study of intermolecular interactions in crystalline arene-perhaloarene adducts in terms of the electron density

*Bruno Landeros-Rivera, Rafael Moreno-Esparza and Jesús Hernández-Trujillo**
Facultad de Química, UNAM, Mexico City, 04510, Mexico. E-mail: jesusht@unam.mx

1 Cristalization

In the crystallization of the hexafluorobenzene-pyrene complex (**1**), 0.3 mmol of pyrene (0.0606 g) 99% where dissolved in 3 ml of hexafluorobenzene 99% after moderate heating and stirring. Because of the lower solubility of triphenylene, only 0.04 mmol of triphenylene (0.0091 g) 98% were dissolved in 2 ml of hexafluorobenzene 99% for the hexafluorobenzene-triphenylene complex (**2**) formation. Air-unstable small needle crystals appeared after slow solvent evaporation in both cases. Both crystalizations were carried out as described by Collings et al.[1]

For the hexachlorobenzene-pyrene complex (**3**) 0.05 mmol of pyrene (0.0101 g) 99% and 0.05 mmol of hexachlorobenzene (0.0142 g) 99.9% were dissolved separately in 2 ml of ethyl ether. When complete dilution was reached under 10 minutes of sonication, both solutions were mixed. After slow solvent evaporation, thin needle crystals were obtained. The same procedure was employed for the formation of the hexachlorobenzene-triphenylene complex (**4**), using the same reagents as for **2** and **3**. In contrast to **1** and **2**, **3** and **4** crystals were stable even outside of mother liquor.

2 X-ray diffraction experiments

All measurements were made with Mo-Kα radiation in an Oxford Gemini Diffractometer. Data reduction was carried out with CrysAlisPro.[2] Structures were solved with Superflip, which is included in the WinGX Program System.[3] SHELX programas[4] with the ShelXle[5] GUI were used for the structural refinements. Constraints over thermal ellipsoids and geometrical parameters. The cell parameters of **1** and **2** agree with the previous reported ones[1] and the atomic positions were only used as input data for theoretical calculations. Low temperature measurements were carried out for **1**, **2** and **4** (100, 130 and 100 K, respectively) but not for **3** because below 240 K it undergoes a phase transition that fractures the crystal.

3 Multipolar refinement of theoretical structure factors

The refinement strategy was as follows: First the scaling factor of the four complexes were refined and the obtained values are close to unity. Then a set of 4 κ parameters for non-hydrogen atoms (one for halogens and three for carbons with the different local symmetry) were refined along with constraints over valence populations of equivalent atoms. The κ parameteres for the H atoms were fixed to 1.16. Next, dipoles, quadrupoles, octupoles and hexadecapoles were refined (each one in different steps) with constraints considering the local symmetry for non-hydrogen atoms. For H atoms only dipoles were refined. Then equivalence between all non-hydrogen atoms was removed. Subsequently, κ' parameters of non-hydrogen atoms were refined (for H atoms these were also fixed to 1.16). Finally, the symmetry constraints were released and all parameters were refined concurrently. The quality of the multipole refinement can be judged by the low values of R1(F) which are 0.0050, 0.0053, 0.0034 and 0.0034 for **1**, **2**, **3** and **4** respectively. Negative peaks with absolute

values no higher than 0.06 and 0.24 e·Å^{-3} were found at fluorine and chlorine nuclei, respectively. Positive peaks are found over each carbon nucleus, which is likely a consequence of the limitation of the multiple refinement to describe the electron density at the nucleus with a frozen core density. Given that this work is about intermolecular interactions, this result represents no complication since these are correctly described because no appreciable residual density is observed in the intermolecular region.

Table S1 Average value of $\nabla^2\rho_b$ (e·Å^{-5}), the electronic energy density H_b (a.u.), potential energy density V_b (a.u.), its ratio with the positive definite kinetic energy density, $|V_b/G_b|$ and the number of BCPs corresponding to each group of interactions in the four complexes.

Contact	$\nabla^2\rho_b$	H_b	V_b	$\lvert V_b/G_b\rvert$	BCPs
1					
$\pi\cdots\pi$	0.447	0.0009	−0.0029	0.77	3
X···H	0.456	0.0013	−0.0021	0.60	9
H···H	0.418	0.0011	−0.0022	0.67	4
X···X	0.170	0.0006	−0.0006	0.54	1
2					
$\pi\cdots\pi$	0.390	0.0008	−0.0032	0.80	6
$\pi\cdots$X	0.390	0.0010	−0.0021	0.68	2
$\pi\cdots$H	0.317	0.0009	−0.0015	0.64	7
X···H	0.472	0.0014	−0.0021	0.57	17
H···H	0.420	0.0011	−0.0022	0.67	3
X···X	0.180	0.0006	−0.0008	0.59	4
3					
$\pi\cdots\pi$	0.313	0.0007	−0.0019	0.73	6
$\pi\cdots$X	0.371	0.0009	−0.0021	0.69	11
X···H	0.455	0.0012	−0.0024	0.64	12
H···H	0.434	0.0011	−0.0024	0.66	7
X···X	0.548	0.0011	−0.0036	0.72	5
4					
$\pi\cdots\pi$	0.407	0.0008	−0.0026	0.77	7
$\pi\cdots$X	0.360	0.0009	−0.0019	0.64	9
$\pi\cdots$H	0.340	0.0009	−0.0017	0.65	4
X···H	0.495	0.0013	−0.0026	0.67	19
X···X	0.256	0.0007	−0.0013	0.65	5

4 Molecular graphs and NCI isosurfaces

The remainder molecular graphs and NCI isosurfaces not shown in the manuscript are depicted in Figure S1 and Figure S2.

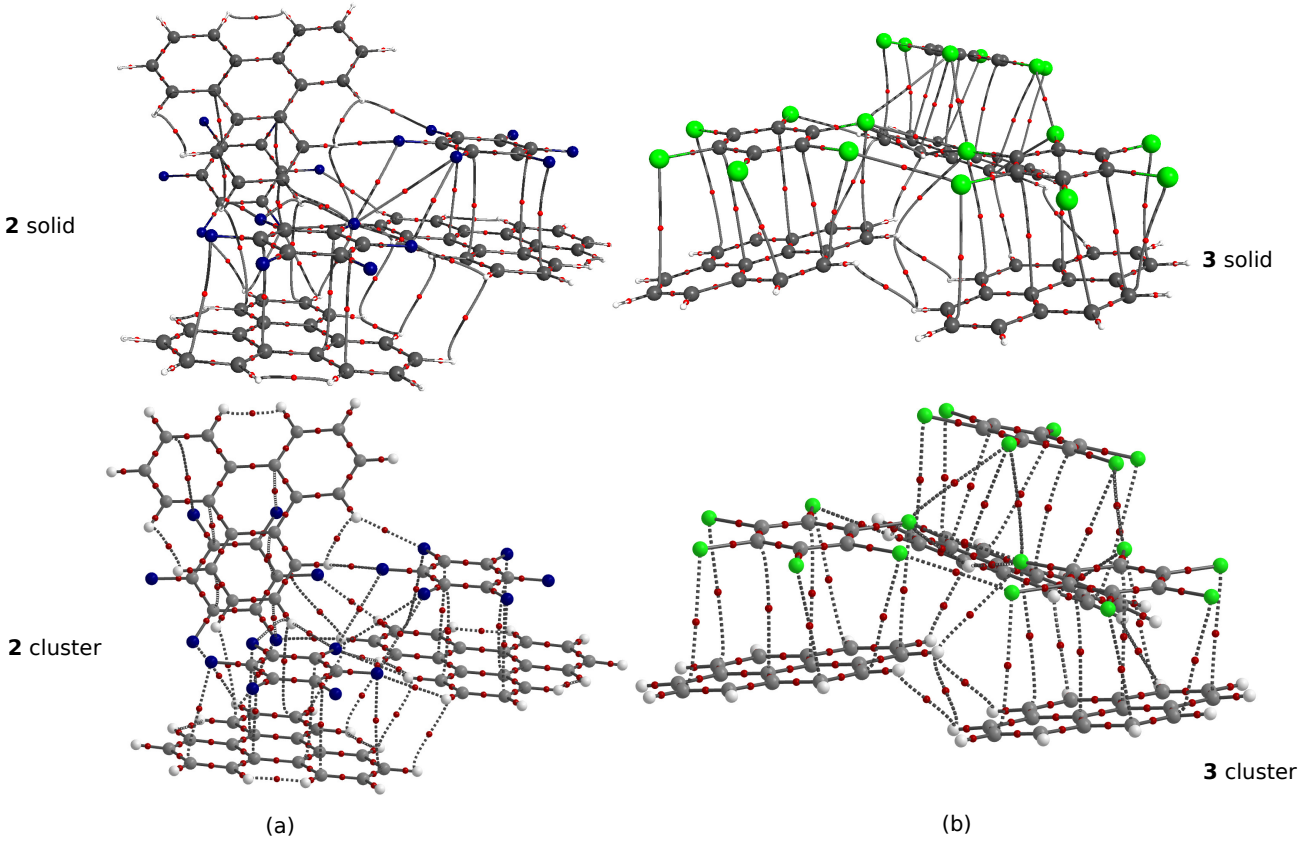

Figure S1. Molecular graphs of (a) **2** and (b) **3** in the solid and in a molecular cluster using the same atomic coordinates. BCPs are depicted in red and bond paths in grey.

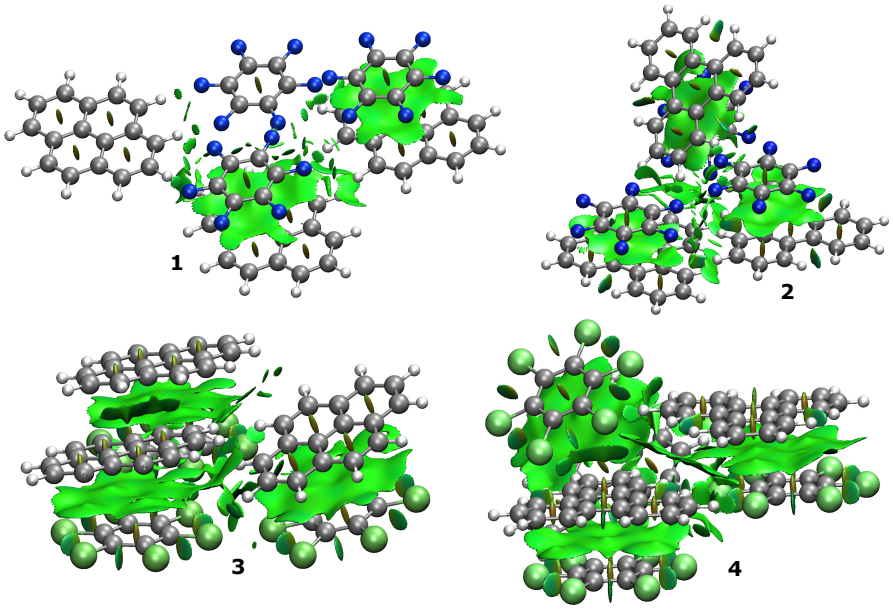

Figure S2. NCI isosurfaces of **1**, **2**, **3** and **4** complexes drawn at 0.5 a.u.

5 Estimate of the cohesive energy with the Espinosa-Molins-Lecomte equation

The cohesive energy is approximated in terms of the potential energy densities at the intermolecular bond critical points, V_b, shared by the molecules A and B in a crystal with their neighbors. Each pair of atoms connected by a bond path contributes with a term $0.5V_{b_i}$, following the Espinosa-Molins-Lecomte equation. A variant for this approximation, where the empirical 0.5 coefficient is changed to 1.0, was proposed for the computation of the cohesion energy (E'_{coh}). For this estimate, all the contacts around each molecule are considered, avoiding double counting, so that $E'_{\mathrm{coh}} = \sum_{b_i} V_{b_i}$. The number of non-equivalent BCPs (NEB) considered in each case depends on the asymmetric unit. For **2** and **4**, there are only one arene and one perhaloarene molecules in the asymmetric unit, therefore each NEB should be considered only once. There are only half molecules in **1**, so each NEB should be counted twice. In the case of **3**, there are 4 half molecules so each NEB should be counted only once.

6 Components of the dimerization energy

Figure S3 depicts the different dimers of **1** used for the calculation of the interaction energy. Analogue complexes were used for the other adducts. The different contributions to the interaction energies for all the dimers are reported in Table S2.

Table S2 Electrostatic, polarization, dispersion and repulsion contributions to the interaction energy calculated for the most stable dimers of different types for **1**, **2**, **3** and **4**. All values in kcal/mol.

Dimer	E_{elec}	E_{pol}	E_{disp}	E_{rep}	E_{tot}
1					
$(C_6X_6)_2$	0.0	0.0	−0.3	0.0	−0.3
$(PAH)_2$	−1.6	−0.6	−4.9	3.5	−3.7
C_6X_6−PAH (stacked)	−3.3	−1.5	−11.5	8.5	−7.8
C_6X_6−PAH (edge-edge)	−0.5	−0.2	−2.0	1.1	−1.6
2					
$(C_6X_6)_2$	−0.1	0.0	−0.6	0.0	−0.7
$(PAH)_2$	−2.2	−0.8	−7.2	4.9	−5.4
C_6X_6−PAH (stacked)	−3.2	−1.6	−12.0	9.3	−7.4
C_6X_6−PAH (edge-edge)	−0.6	−0.2	−2.2	1.3	−1.8
3					
$(C_6X_6)_2$	−0.5	−0.3	−2.9	1.8	−1.9
$(PAH)_2$	−1.4	−0.7	−4.6	3.2	−3.5
C_6X_6−PAH (stacked)	−3.4	−1.6	−17.9	10.6	−12.4
C_6X_6−PAH (edge-edge)	−1.8	−1.2	−4.7	4.9	−2.9
4					
$(C_6X_6)_2$	−0.3	−0.1	−2.7	1.1	−2.0
$(PAH)_2$	−1.7	−0.6	−6.3	3.4	−5.2
C_6X_6−PAH (stacked)	−4.2	−2.0	−21.9	14.3	−13.9
C_6X_6−PAH (edge-edge)	−1.3	−0.8	−5.1	3.1	−4.0

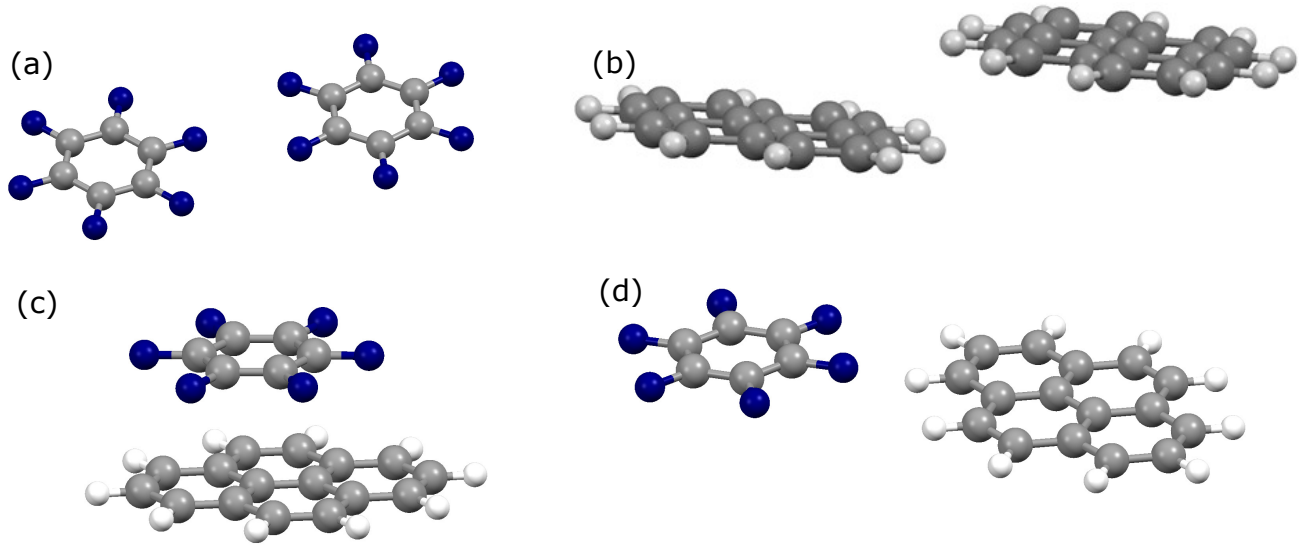

Figure S3. (a) $(C_6X_6)_2$, (b) $(PAH)_2$, (c) C_6X_6-PAH (stacked) and (d) C_6X_6-PAH (edge-edge) dimers of **1**.

References

[1] J. C. Collings, K. P. Roscoe, E. G. Robins, A. S. Batsanov, L. M. Stimson, J. A. K. Howard, S. J. Clark and T. B. Marder, *New J. Chem.*, 2002, **26**, 1740–1746.

[2] *CrysAlisPRO, Oxford Diffraction /Agilent Technologies UK Ltd, Yarnton, England.*

[3] L. J. Farrugia, *J. Appl. Crystallogr.*, 2012, **45**, 849–854.

[4] G. M. Sheldrick, *Acta Crystallogr., Sect. C*, 2015, **71**, 3–8.

[5] C. B. Hübschle, G. M. Sheldrick and B. Dittrich, *J. Appl. Crystallogr.*, 2011, **44**, 1281–1284.